

RSCPublishing PCCP

**Molecular dynamics simulations of the water adsorption  
around malonic acid aerosol models**

Journal:	<i>Physical Chemistry Chemical Physics</i>
Manuscript ID:	CP-ART-02-2013-050608.R1
Article Type:	Paper
Date Submitted by the Author:	n/a
Complete List of Authors:	DARVAS, Maria; SISSA, PICAUD, Sylvain; Institut UTINAM - UMR 6213, UTINAM-B Jedlovsky, Pal; Eötvös Loránd University, Institute of Chemistry

SCHOLARONE™  
Manuscripts

# Molecular dynamics simulations of the water adsorption around malonic acid aerosol models

Maria Darvas<sup>[a,b,c]</sup>, Sylvain Picaud,<sup>\*[a]</sup> Pál Jedlovszky<sup>[b,d,e]</sup>

- [a] M. Darvas, Dr. S. Picaud  
Institut UTINAM – UMR 6213 CNRS  
Université de Franche-Comté  
16 route de Gray, F-25030 Besançon Cedex, France  
E-mail: sylvain.picaud@univ-fcomte.fr
- [b] M. Darvas, P. Jedlovszky  
Laboratory of Interfaces and Nanosized Systems, Institute of Chemistry,  
Eötvös Loránd University  
Pázmány Péter stny. 1/a, H-1117 Budapest, Hungary
- [c] M. Darvas,  
Sector of Statistical and Biophysics  
Scuola Internazionale Superiore di Studi Avanzati  
via Bonomea, 265, 34136 Trieste, Italy
- [d] P. Jedlovszky  
MTA-BME Research Group of Technical Analytical Chemistry,  
Szt. Gellért tér 4, H-1111, Budapest, Hungary
- [e] P. Jedlovszky  
EKF Department of Chemistry,  
Leányka u. 6, H-3300 Eger, Hungary

## Abstract.

Water nucleation around a malonic acid aggregate has been studied by means of molecular dynamics simulations in the temperature and pressure range relevant for atmospheric conditions. Systems of different water contents have been considered and a large number of simulations has allowed us to determine the phase diagram of the corresponding binary malonic acid–water systems. Two phases have been evidenced in the phase diagrams corresponding either to water adsorption on a large malonic acid grain at low temperatures, or to the formation of a liquid-like mixed aggregate of the two types of molecules, at higher temperatures. Finally, the comparison between the phase diagrams simulated for malonic acid–water and oxalic acid–water mixtures emphasizes the influence of the O:C ratio on the hydrophilic behavior of the aerosol, and thus on its ability to act as a cloud condensation nucleus, in accordance with recent experimental conclusions.

## 1. Introduction

The interactions between water and organic molecules receive much attention because of their particular importance in biology and technology. More recently, these interactions have also been investigated in the context of atmospheric chemistry [1,2] because it has been recognized that ice particles may scavenge some of these organic molecules from the atmosphere, thus modifying both the atmospheric composition and the atmospheric chemistry. [3] Another field of interest deals with the interaction of water molecules with organic aerosols (see, for instance, Ref. 4). Indeed, a large amount of volatile organic compounds (VOCs) are emitted into the atmosphere each day, from both natural sources and anthropogenic activities, which are then involved in aerosol formation after oxidation or direct aggregation.[5] These aerosols play a central role not only in the health effects of air pollution but also on climate evolution.[6,7] Indeed, they have both a direct effect on climate by scattering light, which results in negative radiative forcing (i.e., cooling), and an indirect effect by acting as cloud condensation (CCN) or ice nuclei (IN), thus changing cloud properties.[6] Aerosols may impact on the number, concentration, and size of cloud droplets and induce changes in the light scattering by clouds, in their lifetimes, and precipitation rates. For all these reasons, a better understanding of the interactions between water and aerosols is urgently needed, aiming at describing in detail the ability of aerosols to act as condensation nuclei for water, either in the liquid (CCN) or in the solid (IN) state. However, the corresponding systems are very complex, mainly because aerosols are mixtures of compounds, and their properties depend strongly on the way of production. In general, the predominant chemical components of air particulate matter are sulfates, ammonium nitrate, sea salt, mineral dust, black carbon and organic compounds, whose relative abundance depends on, e.g., location, time, and meteorological conditions.[6]

Owing to the complexity of the aerosol surface chemistry,[8] modeling ideal systems by computer simulations is an interesting way to achieve a better description of the water-aerosol interactions at the molecular scale. **A growing number of simulation studies have thus been devoted to the characterization of the interactions between water molecules and aerosols but only a few of them have been specifically devoted to organic aerosols or organic surfaces.[2, 9-25]** In contrast, such approaches have been widely used for ten years to describe the interactions between organic compounds and ice surfaces in the atmosphere, either based on *ab initio* calculations [26-29] or on classical simulations (Monte Carlo and molecular dynamics),[30-43] and it has been shown that these simulations led to a rather satisfactory agreement with experimental data [32-34, 38-41, 43] or *in situ* observations.[36]

While most of these studies focused on quite simple organic molecules, we recently used molecular dynamics simulations to characterize the details of the interaction between ice surfaces and more complex, difunctionalized molecules, such as hydroxyacetone [40] and oxalic acid.[44] In particular, the latter molecule has been used as a model for dicarboxylic acid molecules adsorption on ice. Indeed, low molecular weight dicarboxylic acids are ubiquitous in the troposphere where their interaction with ice particles should be characterized. The fair agreement between the simulation results and the available experimental data [45] gave us confidence in the potential model used to calculate the acid-water interactions and we then used the same potential model to perform the first molecular dynamics simulation study of the water adsorption around oxalic acid aggregates used as surrogate for organic aerosols.[46] Indeed, dicarboxylic acids represent about 30-50 % of the total organic particulate matter in the troposphere, and they are thus major components of organic aerosols. Here, we go beyond this first study by considering the larger malonic acid molecule, aiming at characterizing, theoretically, the effect of one additional  $\text{CH}_2$  group (with respect to oxalic acid) on water adsorption. This approach can be related to the very recent experimental work of Schill and Tolbert,[47] who tried to provide simple parametrizations of organic ice nucleation efficacy by using the O:C ratio as a proxy for characterizing the organic aerosol hydrophilicity. It can be also related to the recent work of Ma et al.,[24] in which molecular dynamics simulations have been performed to characterize dicarboxylic coated aqueous aerosols. However, in this case, the simulations considered big water droplets coated by dicarboxylic acid molecules, whereas in our approach, we characterize the reverse situation, i.e., big acid aggregates interacting with surrounding water molecules.

## 2. Computational details

Molecular dynamics simulations of the formation and stability of malonic acid aerosols together with the adsorption of water on the aerosol particles at two different compositions have been performed using the GROMACS simulation program package.[48] Simulations of the neat malonic acid aerosol were carried out on the canonical ( $N, V, T$ ) ensemble at 200 K. The adsorption of water on an aerosol particle was modelled in the isothermal-isobaric ensemble at six different, atmospherically relevant pressure values ranging between 0.01 and 1 bar, and six temperatures between 100 and 250 K. The temperature and pressure of the systems were controlled by means of the weak coupling algorithm of Berendsen et al.[49] An integration time step of 1 fs was used in each of the molecular dynamics runs. For three randomly chosen temperature-pressure pairs calculations have been repeated using the Nosé-Hoover thermostat [50,51] and the Parrinello-Rahman barostat [52] to examine the possible effect of the choice of temperature and pressure

coupling algorithms on the results. The results obtained with different coupling methods turned out to be in good agreement with each other.

**As in our previous studies, [44,46] water molecules** were described by the TIP5P model.[53] The initial geometry and the potential parameters of the malonic acid molecules were taken from the OPLS library.[54] Water molecules were fully rigid, while bond angle and torsional flexibility was allowed for the malonic acid molecules. The geometry of water, and bond lengths of the malonic acid molecule were kept fixed by means of the SETTLE [55] and LINCS [56] algorithms, respectively. The potential energy of the systems investigated was calculated as the sum of the atom-atom pairwise interaction energies between the interacting species. The interaction energy between an atom pair was calculated as the sum of the dispersion-repulsion and Coulomb terms acting between two of the atoms and their partial charges. The dispersion-repulsion terms were calculated with the usual Lennard – Jones (6-12) potential. The Lennard-Jones  $\sigma$  and  $\varepsilon$  parameters of the corresponding atom pairs were obtained from the  $\sigma$  and  $\varepsilon$  values of the individual atoms according to the Lorentz-Berthelot rules.[57] The Lennard-Jones interactions were neglected for atom pairs positioned at distances larger than the cut-off distance of 9 Å. The long-range part of the electrostatic interactions was taken into account by the Particle Mesh Ewald (PME) [58] method beyond the same molecule centered cutoff value. For the sake of a more clear analysis we have repeated some of the simulations without periodic boundary conditions, to ensure that the obtained results are meaningful and do not originate from any possible artefact resulting from translational periodicity, more precisely, from an unphysical confinement of water molecules between periodic images of the aerosol particles.

To create the malonic acid aerosol we have placed a nucleus consisting of 5 malonic acid molecules in the middle of a cubic simulation box, having an edge length of 54.5 Å, to serve as a nucleation core, around which 120 more malonic acid molecules were placed randomly. This initial system was equilibrated by a 1 ns long simulation on the  $(N,V,T)$  ensemble at 200 K. During the course of this run the malonic acid molecules aggregated to form one big aerosol particle in equilibrium with some monomers. Once the aerosol was formed, an equilibration run of 5 ns, performed under the same conditions has been launched. Simulations have been repeated with a system of double density, consisting of 240 randomly placed malonic acid molecules and the nucleation grain to check the dependence of the formed aerosol on the initial density of the system. It has been found that, unlike what had been reported in our previous paper on oxalic acid aerosols,[46] in the malonic acid case the size of the aerosol depended on the initial density of the system, thus for the double density we obtained a stable aerosol twice as big as for the lower density case. This particle consisted of 212 malonic acid molecules, being in equilibrium with monomers

and dimers. The largest stable aggregate was taken as a model of an aerosol particle for our further studies devoted to the investigation of adsorption of water on a malonic acid nucleus.

In order to ensure the credibility of the above mentioned dependence of the cluster size on the initial density of the system, the following tests have been performed. Primarily, the simulations have been repeated with 360, 480 and 600 malonic acid molecules added to the original small nucleus to assess the upper limit of the range in which the cluster size is a function of the density. It has been found that this dependence stands even at the highest initial density (600 malonic acid molecules). To be able to exclude the possibility of a finite size effect simulations have also been repeated with an initial box size characterised by an edge length of 150 Å, which means a more than twenty-fold increase in the box volume, and the same effect has been observed. It thus appears that malonic acid molecules, unlike oxalic acid, have a strong tendency to form very large aggregates. However, we have chosen to work with the above mentioned aggregate of 212 malonic acid molecules, which appeared as a good compromise between the relevance and the time cost of the corresponding simulations.

Two different compositions have been chosen to investigate the adsorption of water on the aerosol and to analyse the phase behavior of the resulting binary systems. The stabilized malonic acid aggregate consisting of 212 molecules has been placed in the middle of an empty cubic simulation box having the edge length of 70 Å. Then, 300 and 1500 water molecules, respectively, have been placed randomly in the basic box, modelling thus roughly 58 and 88 mole % water content. Both systems have been equilibrated primarily on the canonical ( $N, V, T$ ) ensemble for 4 ns at a temperature as low as 100 K. The pre-equilibrated systems have then been further equilibrated for 1 ns with an integration time step of 1 fs on the isothermal-isobaric ( $N, p, T$ ) ensemble at 6-6 different, atmospherically relevant temperature and pressure values, respectively. Each of these simulations has been followed by a 1 ns long production run, performed under the same conditions, during which 1000 equilibrium configurations, separated by 1 ps long trajectories each have been saved for the analyses.

A total number of 36 simulations for each composition have thus been performed to reconstruct the phase behavior of the binary malonic acid-water system. In such binary mixtures, the structural characteristics are well visible by looking at equilibrium snapshots, or as a more quantitative approach, they might be investigated by means of detailed cluster analysis. Binding energy distributions, on the other hand, are useful tools to provide us with information about the hydrogen bonded network of the aerosol. We have thus calculated the  $P(n)$  distribution of the size of the

malonic acid clusters disregarding the water molecules, that of the water clusters without the malonic acid molecules, and also the cluster size distributions taking both components into account for all the pressure-temperature pairs considered at both compositions. During the course of this analysis two malonic acid molecules have been regarded to be hydrogen bonded if the distance from any of their hydrogens to any of the hydroxylic or carboxylic oxygen atoms of the other malonic acid molecule was smaller than a cut-off distance of 2.45 Å or 3.50 Å respectively. The distance between the carboxylic and hydroxyl oxygen atoms had to be smaller than a cut-off value of 4.60 Å and the hydroxyl O - hydroxyl O distance had to be smaller than 3.50 Å. A water and a malonic acid molecule have been considered to be connected by a hydrogen bond if the H(acid) – O(water) and the hydroxyl O(acid) – O(water) cut-off distances turned out to be smaller than the cut-off values of 2.65 Å and 3.50 Å, respectively. In the same way, two water molecules have been considered to be hydrogen-bonded neighbors if the distance between their oxygen atoms did not exceed the value of 3.3 Å, while the smallest of the possible oxygen-hydrogen distances has also been smaller than 2.45 Å. The cut-off values listed above have been obtained as the first minimum position of the corresponding partial pair correlation functions. **Based on these hydrogen bond definitions we could identify hydrogen bonded clusters in the system simply as assemblies of molecules in which any molecule pair is connected to each other *via* a chain of hydrogen bonded pairs.** Moreover, to get a deeper insight into the energetic changes that occur during and as a result of the phase transitions, and furthermore, to shed light on the energetic reasons underlying the changes in the characteristics of the different parts of the phase diagram, we have calculated the distributions of the binding energy between a water molecule and all the other waters ( $E_{\text{wat-wat}}^{\text{b}}$ ), between a malonic acid molecule and all the water molecules ( $E_{\text{mal-wat}}^{\text{b}}$ ), and between a malonic acid molecule and all the other malonic acids in the system ( $E_{\text{mal-mal}}^{\text{b}}$ ). The results concerning the phase behaviour, the structural and energetic characteristics are interpreted in comparison with our previous results obtained for oxalic acid-water binary aerosols [46] to get a deeper insight into the possible relation between the carbon atom number (or the O:C ratio) and the ability of the aerosol to act as a cloud condensation nucleus.

### 3. Results and discussion

#### 3.1. Structure of pure aerosol particles

Simulation of the pure aerosol phase of malonic acid molecules resulted in the formation of one big spherical aerosol particle, whose size depends on the initial density, and a few monomers in

equilibrium with the big cluster. This result differs greatly from what had been observed previously for oxalic acid, in which case a strongly polydisperse system had been formed with a maximum cluster size of 60 molecules, regardless of the initial density. In the case of the neat malonic acid aerosol phase thus the equilibrium cluster size depends on the initial concentration (at least, in the present conditions of the simulations), whereas for oxalic acid the size distribution in the observed (atmospherically relevant) density range had been found to be concentration independent. More importantly, a much bigger average aerosol size is found for malonic acid. For the smaller average initial density we have found an equilibrium cluster size of about 100 malonic acid molecules, whereas for the larger initial concentration the aerosol in equilibrium with the remaining monomers consisted of, on average, 210 molecules. The characteristic size of the aerosol particles, and hence also the number of nuclei formed at the same initial density may be an important factor in the efficacy of the aerosol as a cloud condensation nucleus. We speculate that the formation of a number of smaller clusters is more advantageous from the point of view of cloud condensation than that of a bigger aggregate whose overall surface area is smaller. This suggestion is in a quantitative agreement with the finding of Schiller and Tolbert,[47] stating that the higher the O:C ratio of the organic molecule is, the more effective is the aerosol as a cloud condensation nucleus. However, this question may be further elaborated by a comparative investigation of the atomistic structure and energetic characteristics of the oxalic acid-water and malonic acid-water binary aerosols. A snapshot of this big malonic aggregate is shown in Figure 1 together with a snapshot of the stable oxalic acid aggregate.

### 3.2. Phase behavior of the binary aerosol

We have reconstructed the atmospherically relevant section of the phase diagram of the binary aerosols formed by oxalic and malonic acid with water. In both cases it turned out to be possible to differentiate unambiguously between the appearing phases by simply looking at the equilibrium snapshots taken from the simulations corresponding to different temperature-pressure pairs. However, we have also performed cluster analysis to support our conclusions by statistically relevant quantitative results. The phase diagram of the malonic acid-water systems [Fig. 2a] turns out to be much simpler than what had been observed previously for the oxalic acid-water mixtures (Fig. 2b and Ref. [46]). First of all, unlike for the oxalic acid-water systems, we have observed no dependence of the  $(p, T)$  phase diagram on the water concentration, at least in the composition range covered by our simulations. The  $(p, T)$  phase diagram of malonic acid-water mixtures consists of two phases and the pressure, just like in the case of oxalic acid, has turned out to be an irrelevant variable concerning its effect over phase transitions. At low temperatures malonic acid forms one



single big aggregate, on which water molecules are adsorbed in the form of small clusters, while for temperatures above 150 K a mixing of the two phases is seen in a manner that does not involve breakage of the original big aggregate. As seen on the equilibrium snapshots in Figure 3, we may identify the demixed phase of the malonic acid-water system with the low temperature demixed phase observed for the oxalic acid-water system,[46] whereas the mixed phase is apparently similar to the liquid-like mixture observed at high water concentrations at intermediate temperatures.[46] Cluster size distributions calculated at four temperatures for the malonic acid-water systems of both compositions are shown in Figure 4. Total cluster sizes are seen in the top panel, whereas the middle and the bottom panels contain size distributions of malonic acid molecules disregarding waters, and of water molecules disregarding malonic acids, respectively. **It is evident from the total cluster size distributions, i.e., the distributions calculated involving both water and malonic acid molecules, that, regardless of the temperature no dissociation of the binary aggregate happens (top panels of Fig. 4). Moreover, it can be observed that, at low water content, the average size of the binary aggregate is definitely broader for higher temperature values due to thermal motions. At high water content, the average size of the binary aggregate slightly increases by about 30 molecules between 150 and 200 K, but due to its large size the thermal fluctuations appear to be less visible on the figure. More importantly, no appearance of any peak in the region of small aggregation numbers is seen (see the upper inset of the figure showing the total cluster size distribution, at 58% water content).** Taking a closer look at the malonic acid cluster size distributions calculated disregarding water molecules we can draw the conclusion that the initial size of the malonic acid aggregate remains also practically intact when temperature is increased. Here a decrease of the mean value of cluster size is seen at higher temperatures, and subsequently the appearance of some monomers and dimers is visible in the snapshots, however their number is statistically irrelevant as they do not appear in the cluster size distribution as peaks at small values of  $n_{mal}$ . It can thus be concluded that the qualitative picture suggested by the equilibrium snapshots, which states that in case of malonic acid-water mixtures the initial aggregate does not dissociate at higher temperatures, is supported by the total cluster size distribution as well as by the size distribution of the malonic acid clusters. The analysis of the size distribution of the water clusters in the binary systems may provide us with more detailed information about the structure of the adsorbed layer, and may also give at least qualitative information about the mechanism of mixing. At lower temperatures, for the lower water concentration a distribution consisting of several peaks of similar intensity can be observed in the water cluster size range between 5 and 30. **This finding, together with the careful analysis of the MD simulation snapshots, indicates that adsorption happens** in a way that small water clusters are trapped on the

surface of the malonic acid aggregate at low temperatures. At higher temperatures the peaks corresponding to larger water clusters gradually disappear, and in the mixed phase water clusters consisting of, on average, 3-5 molecules are predominant. Such small aggregates of water can more easily penetrate into the voids of the malonic acid aerosol. Thus, the following mixing scheme can be suggested. At higher temperatures water clusters consisting originally of 20-30 molecules break up into smaller ones. At the same time, more intensive thermal motion of the malonic acid molecules initiates the formation of relatively big and flexible voids within the core of the aggregate, allowing the small water clusters to penetrate into the core of the aggregate and fill the voids. We should note here that at the higher water concentration considered this tendency is partially washed out by the fact that here water molecules are present in a sufficient amount to form a percolating network. This network is situated around the malonic acid core at low temperature values. On the other hand, similarly to what has been observed for the system of lower water content, the appearance of quite high-intensity peaks can also be seen at small aggregation number values (**see the lower inset of Fig.4**). This finding suggests a mixing mechanism similar to what has been described for the low concentration case. This would also be in accordance with the fact that malonic acid and total cluster size distributions behave very similarly in both compositions considered. It should also be emphasized that the mixing mechanism suggested simply by looking at the distribution of cluster sizes **is quite speculative**, and one has to investigate the energetic background to get a justification, and to have an at least semi-quantitative picture of the processes underlying the occurring phase transitions.

### 3.3. Energetic background

The binding energy distributions calculated in the malonic acid-water mixed aerosols are presented in Figure 5. Here, the term ‘binding energy’ means the total interaction energy of a certain molecule with all the molecules of a certain kind in the system. **In other words, this is the energy cost of bringing this molecule at infinite distance from the other molecules considered in the energy calculations.** The top, middle, and bottom panels of Fig. 5 show the distribution of the binding energy of a water molecule with the other waters, that of a malonic acid molecule with all the waters, and that of a malonic acid molecule with all the other malonic acids in the system. First of all we should note that, just like in the case of the cluster size distributions, binding energies are not affected significantly by the concentration of water in the system, thus, it is sufficient to analyze the results obtained **for the lower water content in detail**. Looking first at the water-water binding energy distributions, **we can see several peaks at every temperature which can be tentatively related to hydrogen bonding. For instance, four peaks are clearly evidenced at 100, 150, and**

200K, situated roughly at the  $E_b$  values of -95, -70, -30 and 0 kJ/mol. Assuming that the average energy of a single hydrogen bond is around -25 kJ/mol when using the TIP5P interaction potential,[53] these four peaks could thus correspond to arrangements in which one water molecule forms (in average) around 4, 3, 1 and 0 hydrogen-bonds with other waters. Note that, calculating the exact numbers of hydrogen bonds per water molecule would, of course, require a rigorous definition of these H-bonds, based on a combination of energy and geometric criteria. The number of H-bonds given here are thus indication, only.

The peak at zero energy obviously comes from the fact that several water molecules (i.e., gas phase monomers) are too far from the other waters to interact considerably with them. The relative intensity of these peaks varies greatly upon increasing the temperature. Thus, lower energy peaks corresponding to the formation of larger number of hydrogen-bonds between a water molecule and its water neighbors gradually decrease and eventually turn into a shoulder at the highest temperature. This suggests that breaking of water-water hydrogen-bonds occurs at higher temperatures. The same picture is seen for the malonic acid-malonic acid binding energy distributions, with the exception that in this case we obtained a very broad distribution that appears to be unimodal. The peak position of this distribution at low temperatures is at -200 kJ/mol, which corresponds to the formation of 8 hydrogen bonds between a malonic acid molecule and its malonic acid neighbors. With increasing temperature the peak position is shifted towards higher energy values; in the mixed phase the maximum of the distribution occurs at -100 kJ/mol, suggesting that in the mixed phase malonic acid molecules loose about half of their hydrogen-bonded malonic acid neighbors. The loss of any kind of hydrogen-bond is an energetically clearly unfavourable process, which can be compensated by the subsequent formation of other ones at these higher temperature state points. This finding is evidenced by examining the temperature dependence of the malonic acid-water binding energy distributions. As is seen in the middle panel of Fig 5, at low temperatures malonic acid-water hydrogen-bonds, although present to some extent, are less likely formed than at higher temperatures, as the peak position of this distribution shifts towards lower (i.e., more negative) energies with increasing temperature. This finding is in good agreement with the observed mixing at temperatures above 150 K.

#### **3.4. The effect of carbon chain length on the phase behaviour, thermodynamic background**

The above described phase behavior differs substantially from what has been observed previously for oxalic acid-water mixtures under exactly the same conditions,[46] which, knowing that these molecules are consecutive elements of the homologous series of dicarboxylic acids, is a

surprising finding. The only difference between these two dicarboxylic acid molecules is that in malonic acid the two carboxylic groups are separated by a methylene group, hence, this group must be the reason for the differences observed in the phase behavior of the two mixtures. **In the case of oxalic acid-water mixtures we have shown that the phase behavior is governed by entropic factors.**[46] **The same argument holds also for the malonic acid-water mixtures. As we argued in our previous paper,[46] the entropic contribution to the Gibbs free energy can be expressed as the sum of three main types of contributions, as**

$$S_{tot} = S_{comp} + S_{orient} + S_{disp}$$

where the subscripts denote the total entropy and its compositional, orientational and dispersion contributions. The compositional term increases upon mixing regardless of the chemical nature of the molecules constituting the binary system, therefore this contribution should not be affected by the change in the carbon atom number. Dispersion always increases the entropy of any system, thus the formation of small dispersed mixed clusters in case of oxalic acid can be attributed to a favorable change in this contribution. On the other hand, in the case of malonic acid-water mixtures this term remains practically intact when crossing the phase boundary, since no dissociation of the aggregate can be observed. This results in a loss of entropy as compared to the case of the systems containing oxalic acid. However, the big malonic acid aggregate is stable both in the mixed and the demixed phases, and its stability may be attributed to the decreased steric repulsion between the two carboxylic groups, the increased flexibility of the malonic acid molecule as compared to oxalic acid, and the subsequent increase in the orientational degrees of freedom. This increased orientational flexibility is due to the presence of the extra CH<sub>2</sub> group that separates the two carboxylic functional groups. All things considered suggest that the loss of the orientational entropy due to the relative rigidity of the molecular structure of oxalic acid is compensated by the increase of the dispersion term due to the formation of small aggregates.

#### 4. Summary and conclusions

The water nucleation around a malonic acid aggregate has been studied by means of molecular dynamics simulations in the temperature range of 100–250 K and in the pressure range relevant for atmospheric conditions. Systems of two different water compositions have been considered and a total number of 72 simulations have been performed, allowing us to simulate the phase diagram of the binary malonic acid–water systems at these compositions. The results of the simulations showed that only the temperature has a strong influence on the phase behavior of the system whereas the effect of pressure and water composition can be considered as being almost totally negligible in this

respect. Two phases have been thus evidenced for the malonic acid–water systems, corresponding either to water adsorption on a large malonic acid grain at low temperatures, or to the formation of a liquid-like mixed aggregate of water and acid molecules, at higher temperatures. The differences obtained with the water/oxalic acid system behavior have been attributed to the larger flexibility of the malonic acid with respect to the oxalic acid molecule due to the presence of an extra methylene group. **Note that some differences between oxalic and malonic acid aerosol behavior has been evidenced experimentally [59] but it is very difficult to make any comparison (even from a qualitative point of view) between these experimental findings and the simulation results obtained here in different temperature range and for different water contents.**

**Similarly, the results of our simulations cannot be directly compared to any field measurements. However, they can be supported by the recent work of Schill and Tolbert,** in which it has been shown that the efficacy of organic aerosols as cloud condensation nuclei is strongly correlated with the ratio of their O and C atoms, or, in other words, to the hydrophilicity of the aerosol.[47] They have demonstrated that aggregates of molecules characterized by a larger O:C ratio act as significantly more efficient cloud condensation nuclei.[47] Here and in our previous work [46] we have analyzed organic aerosols with two different O:C ratio values, i.e., 2 for oxalic acid and 1.33 for malonic acid. The above finding of Schill and Tolbert [47] is in clear accordance with our results, showing that at atmospherically relevant temperatures oxalic acid-water binary aerosol consists of much smaller grains than what has been observed for malonic acid-water aerosols. The numerous smaller aggregates, either mixed or demixed, have a much bigger total specific surface area than one single, nearly spherical grain, and hence can act as more efficient cloud condensation nuclei. Thus, the origin of the decrease of efficacy of the aerosol particle to act as cloud condensation nuclei within the homologous series of dicarboxylic acids can be understood on the basis of our molecular simulations.

## **Acknowledgment**

M.D.'s PhD was partly granted by the French Government which is gratefully acknowledged. This work was supported by the French Ministry of Higher Education and Research and by the CNRS through the LEFE/CHAT program and by the Hungarian OTKA foundation under project No. 104234. We also acknowledge financial support from the Observatoire des Sciences de l'Univers THETA Franche-Comté-Bourgogne, France. Simulations have been executed on Institut UTINAM's computers supported by the Region de Franche-Comté and the CNRS (Institut des Sciences de l'Univers – INSU).

## References

- 1 Y. Rudich, I. Benjamin, R. Naaman, E. Thomas, S. Trakhtenberg, R. Ussyshkin, *J. Phys. Chem. A*, 2000, **104**, 5238.
- 2 S.G. Moussa, T.M. McIntire, M. Szöri, M. Roeselova, D.J. Tobias, R.L. Grimm, J.C. Hemminger, B.J. Finlayson-Pitts, *J. Phys. Chem. A*, 2009, **113**, 2060.
- 3 J.H. Seinfeld, S.N. Pandis, *Atmospheric Chemistry and Physics*, 2<sup>nd</sup> Edition (Wiley, New York, 2006).
- 4 B.J. Finlayson-Pitts, *Phys. Chem. Chem. Phys.*, 2009, **11**, 7760.
- 5 A.H. Goldstein and I.E. Galbally, *Environ. Sci. Technol.*, 2007, **41**, 1514.
- 6 U. Pöschl, *Angew. Chem. Int. Ed.*, 2005, **44**, 7520.
- 7 M. Kanakidou, J.H. Seinfeld, S.N. Pandis, I. Barnes, F.J. Dentener, M.C. Facchini, R. Van Dingenen, B. Ervens, A. Nenes, C.J. Nielsen, E. Swietlicki, J.P. Putaud, Y. Balkanski, S. Fuzzi, J. Horth, G.K. Moortgat, R. Winterhalter, C.E.L. Myhre, K. Tsigaridis, E. Vignati, E.G. Stephanou, and J. Wilson, *Atmos. Chem. Phys.*, 2005, **5**, 1053.
- 8 K.T. Valsaraj, *Open Journal of Physical Chemistry*, 2012, **2**, 58.
- 9 **J. Hautman, M.L. Klein, *Phys. Rev. Lett.*, 1991, **67**, 1763**
- 10 **Y. Rudich, I. Benjamin, R. Naaman, E. Thomas, S. Trakhtenberg, R. Ussyshkin, *J. Phys. Chem. A*, 2000, **104**, 5238.**
- 11 **J. Chanda, S. Chakraborty, S. Bandyopadhyay, *J. Phys. Chem. B*, 2005, **109**, 471**
- 12 **J.S. Li and G. Wilemski, *Phys. Chem. Chem. Phys.*, 2006, **8**, 1266.**
- 13 **P. Chakraborty and M.R. Zachariah, *J. Phys. Chem. A*, 2007, **111**, 5459.**
- 14 **F. Moulin, S. Picaud, P.N.M. Hoang, P. Jedlovszky, *J. Chem. Phys.*, 2007, **127**, 164719.**
- 15 **P. Chakraborty and M.R. Zachariah, *J. Phys. Chem. A*, 2008, **112**, 966.**
- 16 **N. Winter, J. Vieceli, I. Benjamin, *J. Phys. Chem. B*, 2008, **112**, 227.**
- 17 **A. Rahaman, V.H. Grassian, C.J. Margulis, *J. Phys. Chem. C*, 2008, **112**, 2109**
- 18 **M. Szöri, D.J. Tobias, M. Roeselová, *J. Phys. Chem. B*, 2009, **113**, 4161.**
- 19 **R.L. Grimm, D.J. Tobias, J.C. Hemminger, *J. Phys. Chem. C*, 2010, **114**, 1570.**
- 20 **M. Szöri, P. Jedlovszky, M. Roesolová, *Phys. Chem. Chem. Phys.*, 2010, **12**, 4604.**
- 21 **Gy. Hantal, S. Picaud, P.N.M. Hoang, V.P. Voloshin, N.N. Medvedev, P. Jedlovszky, *J. Chem. Phys.*, 2010, **133**, 144702.**
- 22 **J. Chowdhary, B.M. Ladanyi, *J. Phys. Chem. A*, 2011, **115**, 6306**
- 23 **X. Li, T. Hede, Y. Tu, C. Leck, H. Ågren, *Atmos. Chem. Phys.*, 2011, **11**, 519**
- 24 **X.F. Ma, P. Chakraborty, B.J. Henz, M.R. Zachariah, *Phys. Chem. Chem. Phys.*, 2011, **13**, 9374.**
- 25 **M. Szöri, M. Roesolová, P. Jedlovszky, *J. Phys. Chem. C*, 2011, **115**, 19165.**
- 26 **F. Marinelli and A. Allouche, *Chem. Phys.*, 2001, **272**, 137.**

- 27 A. Allouche, *J. Chem. Phys.*, 2005, **122**, 234703.
- 28 C. Thierfelder and W.G. Schmidt, *Phys. Rev. B*, 2007, **76**, 195426.
- 29 S.M. Hammer, R. Panisch, M. Kobus, J. Glinnemann, M.U. Schmidt, *CrystEngComm*, 2009, **11**, 1291
- 30 S. Picaud and P.N.M. Hoang, *J. Chem. Phys.*, 2000, **112**, 9898.
- 31 B. Collignon and S. Picaud, *Chem. Phys. Lett.*, 2004, **393**, 457.
- 32 N. Peybernès, S. Le Calvé, P. Mirabel, S. Picaud, P.N.M. Hoang, *J. Phys. Chem. B*, 2004, **108**, 17425.
- 33 S. Picaud, P.N.M. Hoang, N. Peybernès, S. Le Calvé, Ph. Mirabel, *J. Chem. Phys.*, 2005, **122**, 194707.
- 34 P. Jedlovszky, L.B. Partay, P.N.M. Hoang, S. Picaud, Ph. van Hessberg, J.N. Crowley, *J. Am. Chem. Soc.*, 2006, **128**, 15300.
- 35 G. Hantal, P. Jedlovszky, P.N.M. Hoang, S. Picaud, *J. Phys. Chem. C*, 2007, **111**, 14170.
- 36 F. Dominé, A. Cincinelli, E. Bonnaud, T. Martellini, S. Picaud, *Environ. Sci. Technol.*, 2007, **41**, 6033.
- 37 G. Hantal, P. Jedlovszky, P.N.M. Hoang, S. Picaud, *Phys. Chem. Chem. Phys.*, 2008, **10**, 6369.
- 38 P. Jedlovszky, G. Hantal, K. Neurohr, S. Picaud, P.N.M. Hoang, Ph. von Hessberg, J.N. Crowley, *J. Phys. Chem. C*, 2008, **112**, 8976.
- 39 M. Petitjean, G. Hantal, C. Chauvin, Ph. Mirabel, S. Le Calvé, P.N.M. Hoang, S. Picaud, P. Jedlovszky, *Langmuir*, 2010, **26**, 9596.
- 40 M. Petitjean, M. Darvas, S. Le Calvé, P. Jedlovszky, S. Picaud, *ChemPhysChem*, 2010, **11**, 3921.
- 41 D. Heger, D. Nachtigallová, F. Surman, J. Krausko, B. Magyarová, M. Brumovský, M. Rubes, I. Gladich, P. Klán, *J. Phys. Chem. A*, 2011, **115**, 11412.
- 42 T.P. Liyana-Arachchi, K.T. Valsaraj, F.R. Hung, *J. Phys. Chem. A*, 2011, **115**, 9226.
- 43 M. Darvas, J. Lasne, C. Laffon, Ph. Parent, S. Picaud, P. Jedlovszky, *Langmuir*, 2012, **28**, 4198.
- 44 M. Darvas, S. Picaud, P. Jedlovszky, *ChemPhysChem*, 2010, **11**, 3971.
- 45 H. Yan and L.T. Chu, *Langmuir*, 2008, **24**, 9410.
- 46 M. Darvas, S. Picaud, P. Jedlovszky, *Phys. Chem. Chem. Phys.*, 2011, **13**, 19830.
- 47 G.P. Schill and M.A. Tolbert, *J. Phys. Chem. A*, 2012, **116**, 6817.
- 48 E. Lindahl, B. Hess, and D. van der Spoel, *J. Mol. Mod.*, 2001, **7**, 306
- 49 H. J. C. Berendsen, J. P. M. Postma, A. DiNola, and J. R. Haak, *J. Chem. Phys.*, 1984, **81**, 3684.
- 50 S. Nosé, *Mol. Phys.*, 1984, **52**, 255.
- 51 W.G. Hoover, *Phys. Rev. A*, 1985, **31**, 1695.
- 52 M. Parinello and A. Rahman, *J. Appl. Phys.*, 1981, **52**, 7182.
- 53 M.W. Mahoney and W.L. Jorgensen, *J. Chem. Phys.*, 2000, **112**, 8910.

- 54 W.L. Jorgensen and J.T. Rivas, *J. Am. Chem. Soc.*, 1988, **110**, 1657.
- 55 S. Miyamoto and P.A. Kollman, *J. Comp. Chem.*, 1992, **13**, 952.
- 56 B. Hess, H. Bekker, H.J.C Berendsen, J.G.E.M. Fraaije, *J. Comp. Chem.*, 1997, **18** 1463.
- 57 M.P. Allen and D.J. Tildesley, *Computer simulations of liquids* (1987, Clarendon Press, Oxford).
- 58 U. Essman, L. Perera, M.L. Berkowitz, T. Darden, H. Lee, L.G. Pedersen, *J. Chem. Phys.*, 1995, **103**, 8577
- 59 C.F. Braban, M. F. Carroll, S.A. Styler, J.P.D. Abbatt, *J. Phys. Chem. A*, 2003, **107**, 6594.



## Captions

**Figure 1:** Top panel shows the molecule models used in the simulations, on the bottom panel equilibrium snapshots of the neat aggregates built up of oxalic (left) and malonic right (right) molecules can be seen.

**Figure 2:** Phase diagram of malonic acid-water (top panel) and oxalic acid-water (bottom panel) binary aerosols. Phase diagrams of both simulated compositions are shown for oxalic acid, whereas for the case of malonic acid-water systems only the smaller water concentration case is shown due to the similarity between the observed phase diagrams of the two simulated compositions

**Figure 3:** Equilibrium snapshots of malonic (left) and oxalic acid (right) binary aerosols formed with water under different physico-chemical conditions; the nomenclature is taken from our previous paper about oxalic acid-water binary aerosols [29]. Phases which were found to be missing in the case of malonic acid-water aerosol systems are crossed out. The insets of the top panels show the aerosol at 150 K to demonstrate the variation of the grain shape due to the increasing temperature.

**Figure 4:** Cluster size distributions of malonic acid-water binary aerosols for 58% (left) and 88% (right) water content at the temperatures of 100 K (black lines), 150 K (red lines), 200 K (green lines), and 250 K (blue lines). Top panels show the total cluster size distributions, including both malonic acid and water molecules, middle panels display the malonic acid cluster size distributions disregarding water molecules, finally water cluster size distributions can be seen on the bottom panels. **Insets of figures are enlargements of some regions of the distribution of particular interest.**

**Figure 5:** Binding energy distributions of malonic acid water binary aerosols for 58% (left) and for 88% (right) water content at the temperatures of 100 K (black lines), 150 K (red lines), 200 K (green lines), and 250 K (blue lines). Top panels: binding energy of a water molecule with all the other waters; middle panels: binding energy between a malonic acid molecule with all the water molecules; bottom panels: binding energy of a malonic acid molecule with all the other malonic acid molecules in the system.

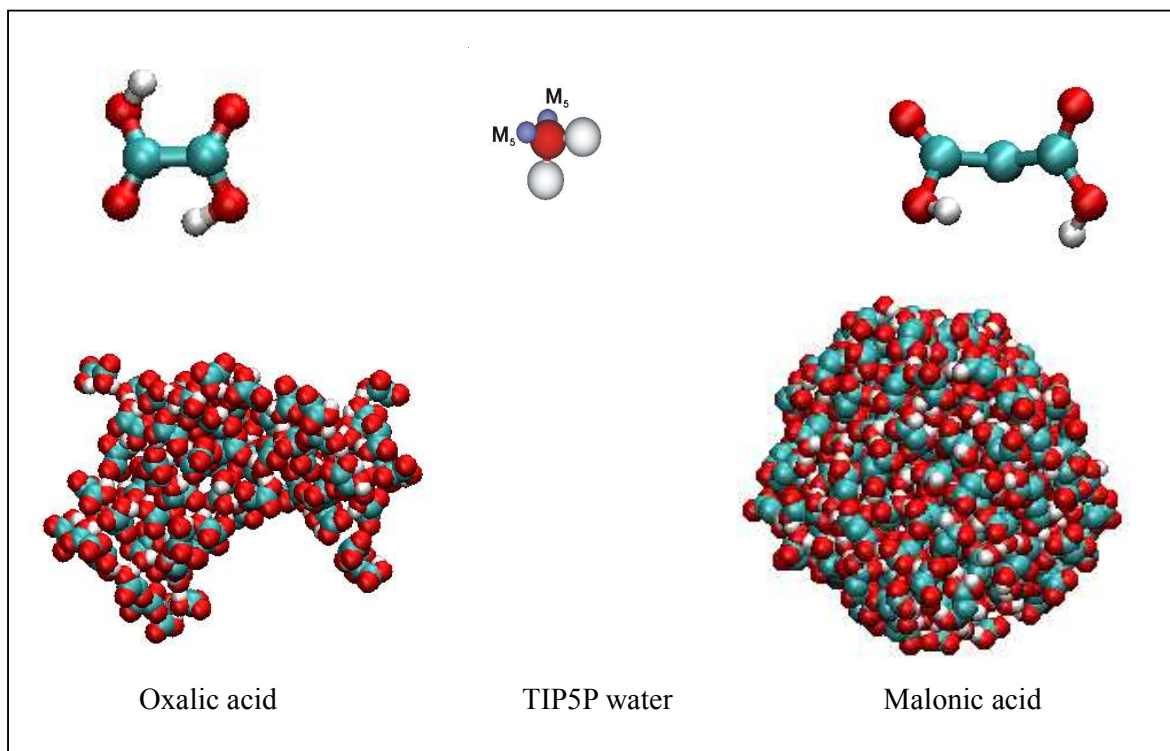


Figure 1

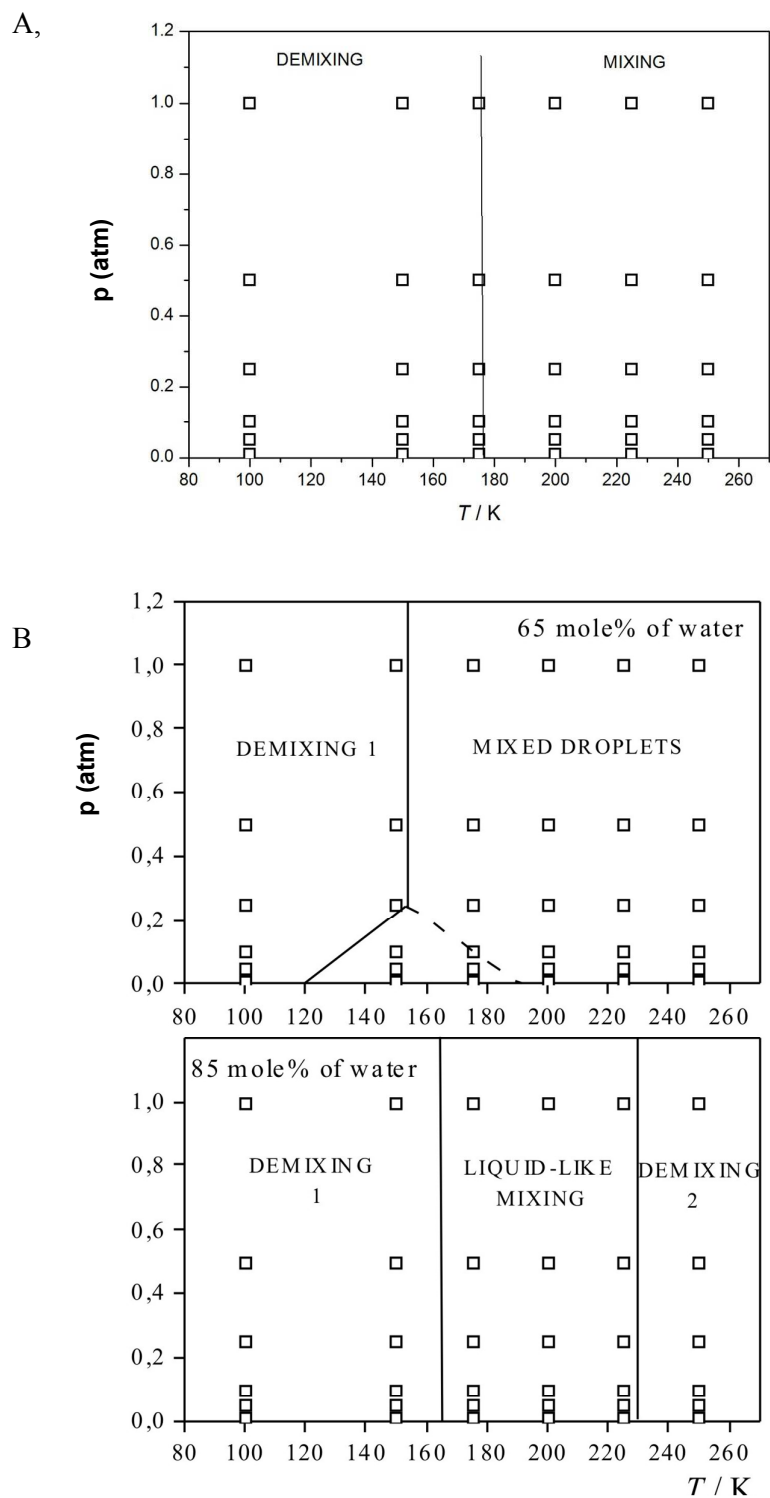
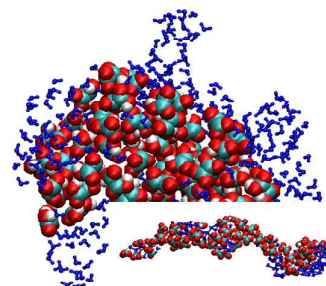
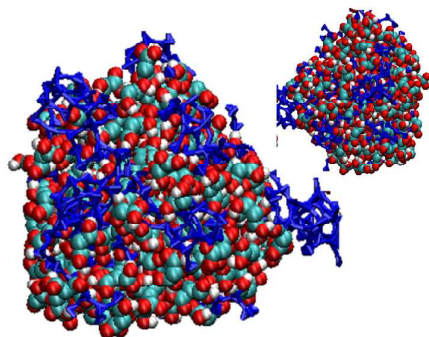
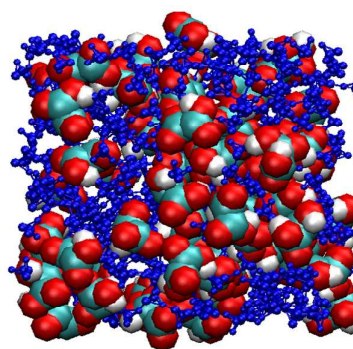
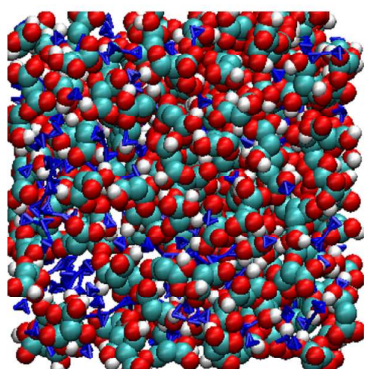


Figure 2

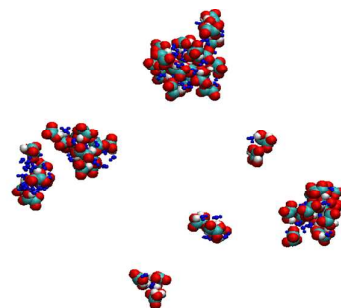
MALONIC ACID

OXALIC ACID

DEMIXING 1

LIQUID-LIKE  
MIXING

MIXED DROPLETS



DEMIXING 2

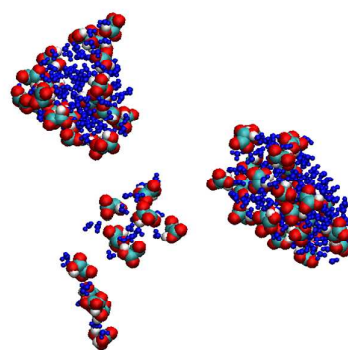


Figure 3

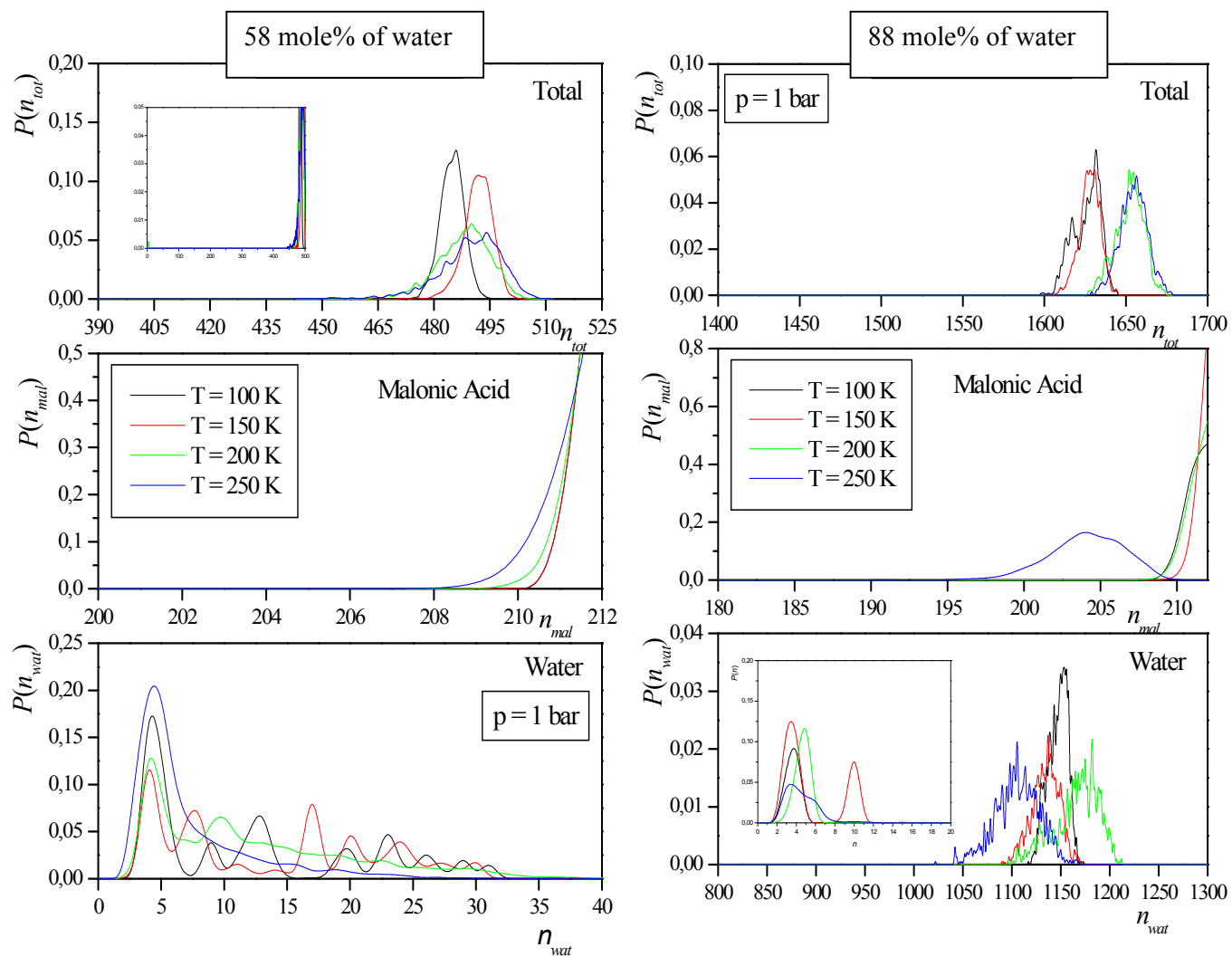


Figure 4

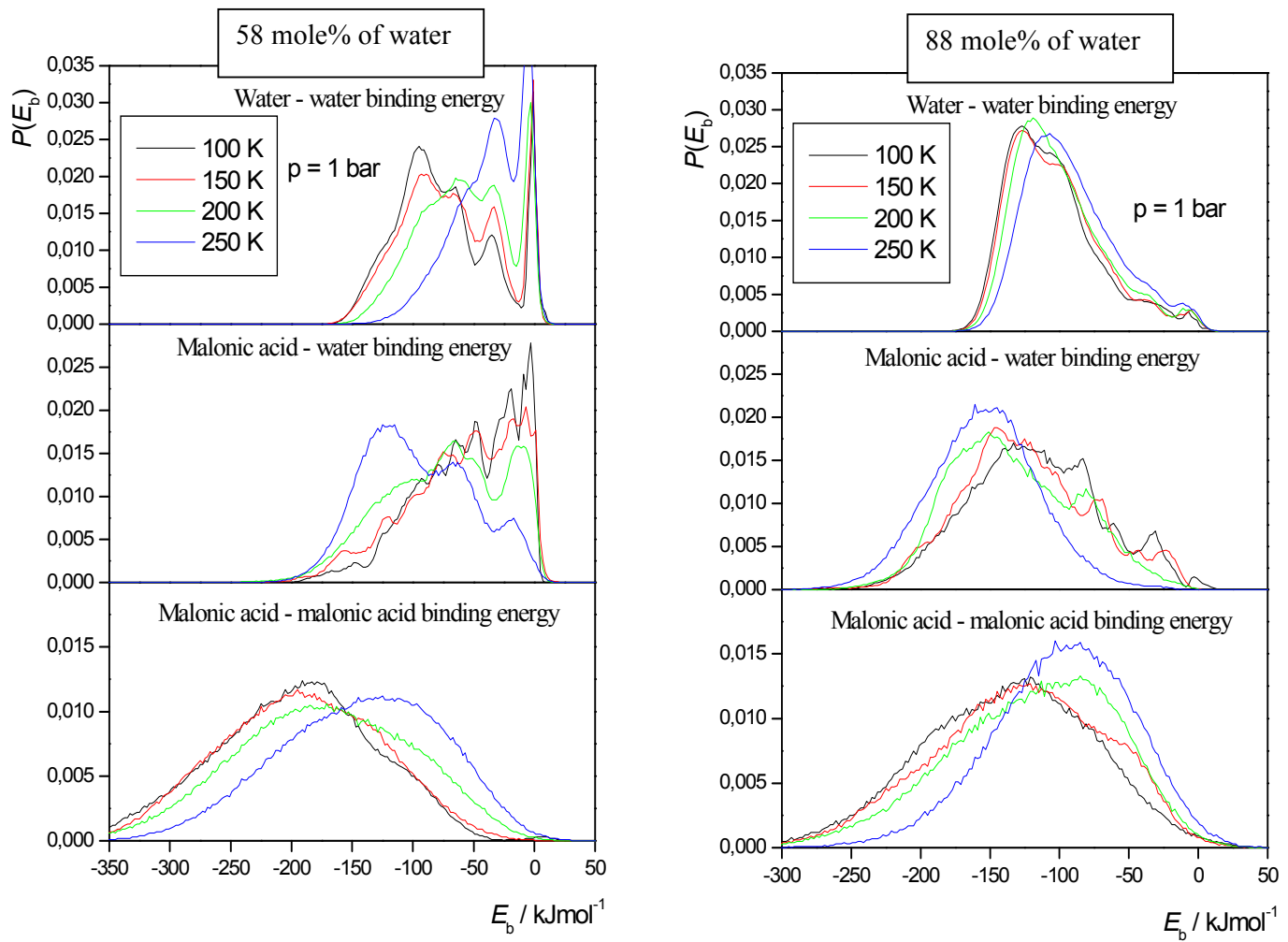


Figure 5

## Reviewer 1

**1. The references to previous computational studies relevant for water – aerosol interactions are limited mostly to studies of organics interacting with ice surfaces (refs 9-26), and the majority of these references are self-citations (11 out of 18). While this may indeed reflect the literature concerning adsorption of organics on ice, it ignores all other computational studies that have addressed the issue of water interaction with organic aerosol surfaces. A more comprehensive overview of previous literature should be included.**

We have included more citations in the Introduction part of the revised paper to take into account this comment.

**2. Significant differences between malonic acid and oxalic acid were observed in the simulations: While oxalic acid forms polydisperse, irregularly shaped clusters with a maximum cluster size of 60 molecules regardless of the initial oxalic acid density in the simulation box, malonic acid exhibits a strong tendency to form very large spherical aggregates. What is known in this regards about the two species from experiment? Is there any experimental evidence of such differences in aggregation between oxalic and malonic acid? Please comment.**

We do not find any experimental study especially focused on this difference. Moreover, the literature on oxalic acid aggregates is very scarce. There is only one paper reporting a comparison study between the phase transitions of malonic and oxalic acid aerosols [Braban et al., J. Phys. Chem. A 107, 6594 (2003)] but it is very difficult to compare the experimental findings (recorded between 252 and 293 K) and our results, although some qualitative agreement can always be found. This has been indicated in the conclusion part of the revised version.

**3. The TIP5P water model was used in combination with the Ewald sum in the present study. The TIP5P model was developed with the spherical cutoff for the electrostatic interactions, and it was shown that it is considerably less accurate if used with other methods for treating long-range interactions. A modified model, TIP5P-Ew, was later developed for the use with the Ewald sum (S. W. Rick, Journal of Chemical Physics 120 (2004) 6085). What was the reason for using TIP5P rather than TIP5P-Ew?**

The main reason for using the TIP5P potential for water is the comparison with our previous study devoted to oxalic acid aggregates which was also based on this TIP5P water potential. We are aware that this potential should rather be used without Ewald sum when calculating some water properties in the [-25°C, +75°C] temperature range [see the paper by Lisal et al., JCP 117, 8892 (2002)]. However, this argument has never been tested at very low temperatures nor for water aggregates of finite size. Moreover, and more importantly, it should be noted that our study is mainly based on the combination between potential parameters of malonic acid and water molecules. Thus, we do not think that the small change between the TIP5P and the TIP5P-Ew parameter values would strongly influence our results.

Nevertheless, to demonstrate that changing from the TIP5P to the TIP5P-Ew water model does not influence our simulation results significantly, we have recalculated the average potential energy and the average coulombic contribution to the energy of the system along one of the trajectories at 88 mole% water concentration (where we suspect that the deviations in the water potential would be more significant due to the larger number of water molecules). The results of this test have shown that the change in the force field for water alters the potential energy by about 0.3 % and the change in the coulombic contribution has turned out to be even smaller. This gives us confidence in the applicability of the TIP5P potential in our simulations.

**4. Top of p. 8: “It can be observed in the top panels of Fig 4 for both concentrations that the average size of the binary aggregate varies slightly with temperature, and the peak is definitely broader for higher temperature values.”**

*(a) There are actually some interesting, albeit small differences between the two top panels: In the case of 88 mole % of water, there seems to be a clear trend, an increase of the total cluster size between the two lower and the two higher temperatures (though the increase by about 50 molecules might very well be unimportant, given the total cluster size of about 1600). Such trend is, however, missing in the 58 mole% case.*

*(b) More importantly, I cannot agree with the second part of the above statement. In the top left panel (58 mole% water), the distributions are indeed broader for  $T = 200$  and  $250$  K than for  $T = 100$  and  $150$  K. However, in the top right panel (88 mole% water), it is NOT the case.*

This point has been clarified in the revised version.

*5. In the last part of section 3.2, the authors say: "This finding allows us to speculate that adsorption happens in a way..." and "...the mixing mechanism suggested simply by looking at the distribution of cluster sizes is highly speculative..." Why "speculate"? In my opinion, it is not necessary to make speculations regarding the mechanism of water adsorption and uptake based merely on the cluster size distributions. It is certainly important to get a more quantitative picture, as the authors provide by analyzing the energetic background. However, the process of water adsorption on the surface of the malonic acid aggregate as well as water penetration in between the malonic acid molecules and formation of the mixed aggregate at higher temperatures can be directly followed in - and confirmed from - the MD simulation trajectories. Does the observed behavior in the simulated malonic acid – water systems support the suggested mechanism? Please elaborate.*

"Speculations" have been made in the paragraph devoted to the analysis of the cluster size distributions, (i.e., they are made only at this point of the paper), because a quantitative picture of the adsorption process requires a more detailed analysis of the energetic backgrounds, of the MD simulation trajectories and of the simulation snapshots, as explained further in the text. We slightly modified the text accordingly.

*6. The adsorption and mixing mechanism, suggested in the manuscript, has been proposed on the basis of the simulation protocol, in which - if I understand correctly - the initial water adsorption on the malonic acid aggregate took place always at 100 K (i.e., during the 4ns NVT equilibration at 100 K after water has been added to the malonic acid aggregate, which was itself pre-equilibrated at  $T = 200$  K), and the temperature was adjusted to the target value (i.e., 100, 150, 200, or 250 K) only subsequently in the NpT production run. Would the authors expect any significant changes in the adsorption and mixing mechanism at higher temperatures if the adsorption was initiated directly at the target temperature rather than at 100 K?*

As indicated on page 5, the acid+water systems have been equilibrated at 100 K on the (N,V,T) ensemble during 4 ns. Then they have been equilibrated at the target temperature on the (N,p,T) ensemble for 1ns before the production run starts. This double step procedure aims at preventing any artificial water/acid mixing at the beginning of the simulations, especially at high temperature.

*7. Discussion of Fig. 5 (lower half of p. 9):*

*(a) "...binding energies are not affected significantly by the concentration of water in the system, thus, it is sufficient to analyze the results obtained for one of the systems in detail." I agree with this statement in general, but there are differences in the level of detail resolved in the energy distributions between the left and right set of panels, which should be discussed.*

*(b) "Looking first at the water-water binding energy distributions, we can see four peaks at every temperature." Although the authors do not specify, which of the two systems (58 or 88 mole% water) they chose to discuss in detail, this sentence suggest it was the system with lower water content, because in the top right panel there are no "four peaks" easily distinguishable. Moreover, it is not true even for all of the distributions in the top left panels, where at the higher temperatures the low energy peaks are suppressed. The wording of the above sentence should be changed.*



(c) *“The four peaks are situated roughly at the  $E_b$  values of -100, -75, -25 and 0 kJ/mol, corresponding to arrangements in which one water molecule forms 4, 3, 1 and 0 hydrogen-bonds with other waters.” I cannot agree with this statement. In the top left panel, there are indeed peaks in the vicinity of  $E_b = 0$  kJ/mol and -100 kJ/mol, but the two peaks in between have maxima clearly different from -75 and -25 kJ/mol (the black and red curves corresponding to 100 and 150 K have actually a minimum at -75 kJ/mol). The authors utilize  $E_b = -25$  kJ/mol as being equivalent to one water – water H-bond. What is the justification? What is the H-bond energy for the TIP5P water model? The results that the authors obtained previously in the oxalic acid – water system correspond very well to this value and, interestingly, also the top right panel of Fig. 5 (malonic acid with 88 mole% water) seems to corroborate this – there are peaks visible in the energy distributions at around 0, -25, -100, and -125 kJ/mol. However, the four peaks in the top left panel (58 mole% water) do not seem to follow the pattern of multiples of 25 kJ/mol. Rather, the four peaks are regularly spaced between 0 and -100 kJ/mol, with the spacing of about 30-35 kJ/mol. This should be addressed in the paper.*

The value of  $E_b = -25$  kJ/mol is estimated from the original paper of Mahoney and Jorgensen for the TIP5P potential [see Fig. 10 of this paper, J. Chem. Phys. 112, 8910, (2000)]. In this paper, the water-water energy distribution of the TIP5P potential is given between 248 and 323 K. The peak position is about -20 kcal/mol (-85 kJ/mol) at 323K, and about -25 kcal/mol (-105 kJ/mol) at 248 K. This agrees very well with the peak of our distribution at 250K and high water contents, indicating that the shift to lower energies is simply an effect of the temperature.

So it is rather crude to assume -25 kJ/mol per hydrogen bond in this distribution (it should be closer to -30 kJ/mol anyway), as there is LJ interaction (repulsion for H-bonded neighbors) and dipole-dipole interaction between all the water pairs, which add a much smaller, but still considerable factor to the binding energy. Further, at room temperature a water molecule has, on average 4.4 nearest (first shell) neighbors, among which 3.6 are H-bonded, the remaining are the so-called interstitial ones. At lower temperatures their number decreases but the H-bonded neighbors increases, decreasing thus the total binding energy.

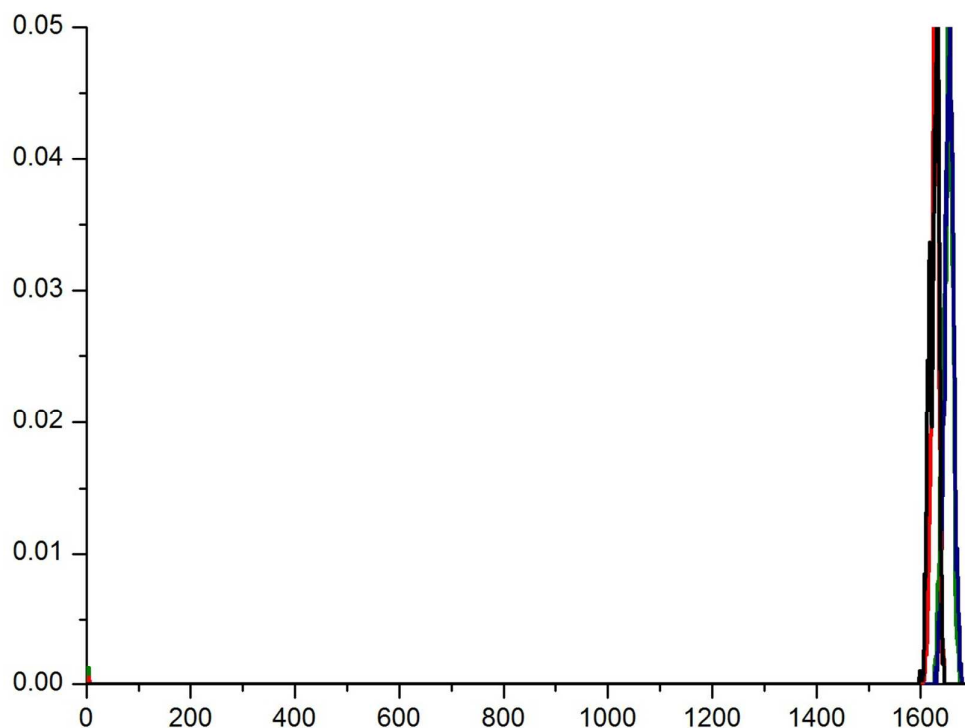
The discussion on the hydrogen bonds is thus quite speculative and a rigorous analysis based also on geometrical criteria should be used to define hydrogen bonds.

The text has been modified accordingly.

Technical:

*It is not quite clear why the inset in the top left panel of Fig. 4 is shown. Also, why isn't a similar inset shown for the 88 mole% water as well? I suppose the inset is to demonstrate that smaller clusters do not appear in any statistically significant amount even at higher temperatures. It would be helpful to elaborate on this little more, perhaps to make a reference to the inset in the text, or at least mention it in the figure caption.*

The inset was shown to demonstrate that smaller clusters do not appear in the corresponding distribution. This has been explained in the text and in the figure caption. A similar inset (see the figure below) is not given at higher water content, because the large scaling (0-1700) of the x-axis combined with the required small size as inset does not provide any visible information in the paper.



***Is the word “tendentious” used correctly? (the first paragraph of section 3.4)***

The corresponding sentence has been modified.

***References need to be corrected - starting from ref. 35, there seems to be a mismatch in the numbering, the numbers in the text do not point to correct papers in the list of references.***

We apologize for this mistake. References have been corrected.

## Reviewer 2

***Specifically: How are the clusters defined? I think that they are determined by hydrogen bond connectivity, since Hbond geometrical criteria are specified, but this is not explicitly stated.***

The clusters have been defined based on connectivity, namely those molecules which have been connected to each other through a continuous network of hydrogen bonds have been regarded as member of the same cluster. This has been indicated in the revised version.

***Binding energies: I assume that these refer to molecules within the same cluster, but this is not specified.***

The binding energies do not refer only to molecules within the same cluster. As indicated in the paper, a specific binding energy is calculated between a molecule (water or acid) and ALL the other molecules of a given type. This is justified for the statistical analysis since we always refer to the same number of molecules (i.e., the total number of molecules) in the energy distributions.

***Regarding these, the sentence on p. 9, 1<sup>st</sup> paragraph of Sec. 3.3, 'In other words, this is the energy cost of bringing the molecule at infinite distance from the others the binding energy of with is considered.' seems garbled and should be clarified/corrected.***

The sentence has been rewritten as: "In other words, this is the energy cost of bringing this molecule at infinite distance from the other molecules considered in the energy calculations".

***The peak position of the binding energy distribution is interpreted as a certain number of H-bonds (bottom of p. 9). Is this reasonable? Presumably, the binding energy includes electrostatic and Lennard-Jones interactions with near and more distant neighbors. In the case of larger mixed clusters, it would have been interesting to include some information on interfacial excess or depletion of the components.***

The peak positions in the binding energy distribution can be used to make only a crude estimation of the number of H-bonds, on the basis of the energy value of one H-bond (average energy between about -20 and -25 kJ/mol, see for instance Mahoney and Jorgensen, J Chem Phys 112, 2000, p. 8910). Of course, to characterize properly these H-bonds, we should have also taken into account geometrical criterion.

A more detailed analysis of the binding energies in terms of interfacial excess or depletion of the components of the distribution would be certainly interesting but it is clearly beyond the scope of the present study.

***It would also have been interesting to indicate if the larger clusters are solid or liquid under a given set of conditions.***

The characterization of the cluster phases is beyond the scope of the paper. Moreover, it would require the definition of unambiguous criteria for defining the liquid or solid state of these clusters (long-range ordering, diffusion coefficients ...). This is not obvious especially for molecular clusters of finite size, see for instance the paper of Egorov et al. Mol. Phys. 100 (2002) 941.

***There are a few typos & stylistic errors***

We thank very much the Reviewer for this list of typos. They have been corrected in the revised version.

## Table of contents

MD simulations of water nucleation around acid aggregates emphasizes the O:C ratio influence on the aerosol hydrophilic behavior.

